Design and Calibration of a Portable 24-GHz 3-D MIMO FMCW Radar with a Non-uniformly Spaced Array and RF Front-End Coexisting on the Same PCB Layer

Zhengyu Peng, Prateek Nallabolu, Changzhi Li
Department of Electrical Engineering, Texas Tech University, Lubbock, Texas, USA. 79409
Email: zpeng.me@gmail.com, prateek-reddy.nallabolu@ttu.edu, changzhi.li@ttu.edu

***Abstract*—This paper presents a portable 24-GHz multiple-input multiple-output (MIMO) radar with 16 transmit (Tx) channels and 16 receive (Rx) channels. The radar is intended for short-range localization and three-dimensional (3-D) imaging by detecting the ranges, azimuth angles, and zenith angles of targets in front of the radar. The radar is capable of two-dimensional (2-D) beamforming achieved using a non-uniformly spaced planar array. A prototype of this 16×16 radar has been built to demonstrate its short-range localization capability.**

***Index Terms*—Frequency-modulated continuous-wave radar, multiple-input multiple-output radar, planar arrays, time-division multiplexing.**

I. Introduction

With the need for more precise and accurate localization and imaging in the internet of things (IoT) era, techniques like multiple-input multiple-output and beamforming are extensively used. The applications of these radars include through-the-wall detection, indoor localization, advanced driver assistance systems, and biomedical applications.

Conventional beamforming techniques include radio frequency (RF) beamforming and digital beamforming. In RF beamforming, each antenna element requires a dedicated phase shifter [1], which inevitably increases the hardware cost and complexity. In digital beamforming [2], each antenna channel requires a high-speed analog-to-digital converter (ADC) or digital-to-analog converter (DAC), thereby increasing the cost and power consumption of the system. To get the range, azimuth angle and zenith angle of a target, a radar system with 2-D beamforming capability is required. Conventional solutions for 2-D beamforming include planar phased array, frequency-scanning array radar [3], synthetic aperture radar (SAR) [4], and multiple-input-multiple-output (MIMO) radar [5]. Planar phased array system requires more antenna elements to achieve good angular resolution. A frequency-scanning array has poor spectrum efficiency since it requires different frequencies to steer the array. A SAR radar requires a mechanical platform to achieve beamforming. A MIMO radar uses lesser number of antenna elements to generate a larger virtual array as compared to the conventional 2-D beamforming architectures.

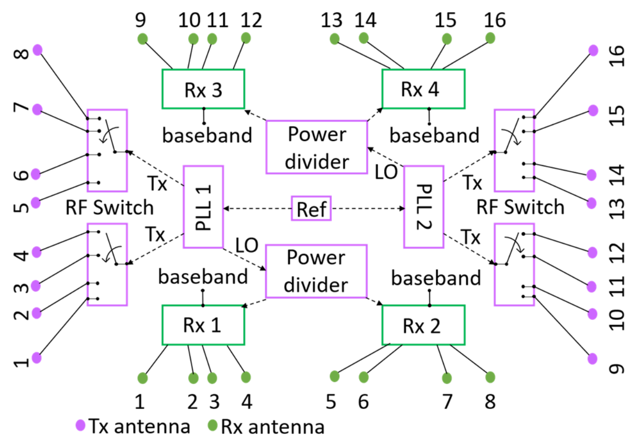

Fig. 1. Block diagram of the RF front-end circuit.

In this paper, a 24-GHz MIMO frequency-modulated continuous-wave (FMCW) radar is designed and tested. The hardware complexity is reduced by employing non-uniformly spaced planar arrays and MIMO concept to achieve 2-D beamforming without having to compromise on the achievable angular resolution. The use of non-uniformly spaced array provides better angular resolution and removes the grating lobe that occurs in a conventional array. The 2-D beamforming together with the radar range detection offer the possibility of 3-D imaging. A 16×16 MIMO radar prototype has been designed and built on a Rogers-3003 substrate. The radar features a Wi-Fi link to transfer the detected baseband data to a personal computer (PC). A calibration method is proposed to align the amplitude and phase of each MIMO channel.

II. Design Concept

The block diagram of the proposed 24-GHz 3-D MIMO radar is shown in Fig. 1. The design includes an RF front-end circuit, which consists of two phase-locked loops (PLL), two voltage-controlled oscillators (VCO), four 24-GHz down-converters, and PIN diodes which acts as RF switches. The VCO and PLL together generate the required FMCW chirp signal and the local oscillator (LO) signal for the down-converters. The transmitting antennas are

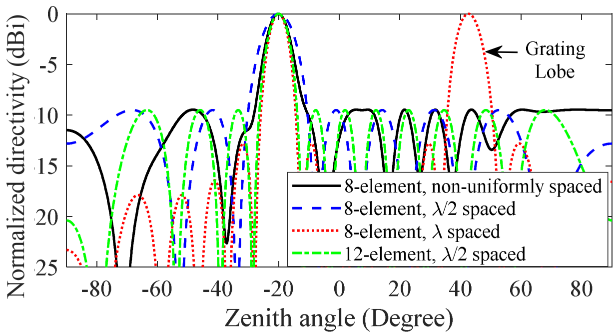

Fig. 2. Comparison of the radiation patterns for four different linear array distributions with the main lobe steered to -20°.

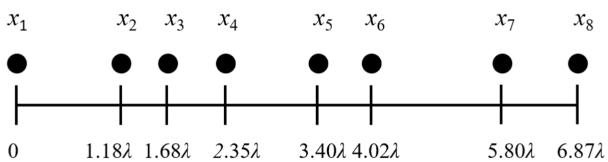

Fig. 3. Distribution of the 8-element non-uniform array.

TABLE I. WEIGHTING VALUES FOR 8-ELEMENT, NON-UNIFORMLY SPACED ARRAY

Element	1	2	3	4
Amplitude	0.3645	0.9685	1	0.7889
Phase (°)	36.36	127.66	0	-131.55
Element	5	6	7	8
Amplitude	0.4371	0.8990	0.6232	0.3411
Phase (°)	-23.28	203.15	157.19	-105.06

vertically distributed, and the receiving antennas are horizontally distributed, both of which use non-uniform spacing to achieve 2-D beamforming. Each PLL has two Tx output channels connected to eight transmitting antennas using RF switches. The down-converter consists of four receive channels which are connected to the receiving antennas. The down-converter converts the received RF signal into baseband which is connected to a baseband board for further processing.

A baseband amplifier amplifies the baseband signal and a 16-channel switch is used to select from one of the 16 baseband signals for further processing. A Wi-Fi chip with built-in ADC is used to transfer the data to a PC. Only one transmitter receiver pair is active at a given time and time-domain multiplexing is used to get data from all the 256 channels.

A. Non-uniformly spaced array

Higher angular resolution can be achieved by using a greater number of antenna elements. Conventional approaches include a linear array with $\lambda/2$ spacing between elements, where λ is the free-space wavelength. The goal of the design is to achieve a trade-off between the aperture size and the number of antenna channels, while maintaining the required beam width and side-lobe level. A comparison is done between 8-element $\lambda/2$ spaced array, 8-element λ spaced array, 8-element non-uniformly spaced array, and 12-element $\lambda/2$ spaced array. Their far-field radiation patterns when the main beam is steered to -20⁰ are shown in Fig. 2. It is observed that 8-element $\lambda/2$ spaced array has the broadest beam width. The 8-element non-uniformly spaced array provides similar beam width as the 12-element $\lambda/2$ spaced array, while maintaining the advantage of 33% reduction in antenna elements. With the same aperture size, the 8-element λ spaced array provides similar beam width and sidelobe level as the non-uniformly spaced array. However, the λ- spaced array suffers from grating lobe issue which can be eliminated using non-uniformly spaced array.

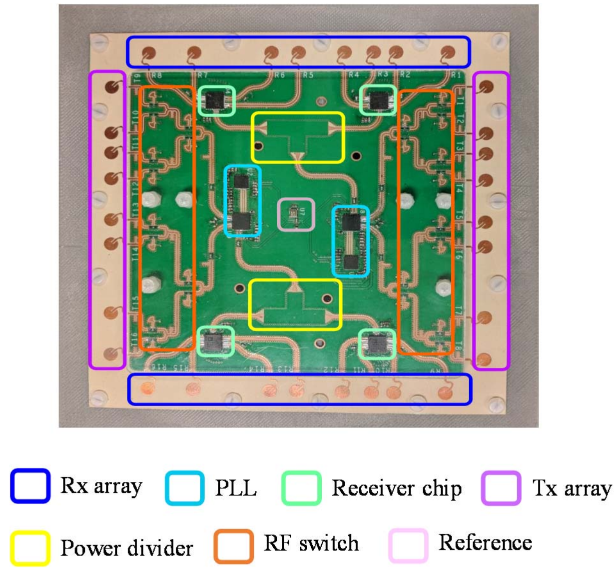

Fig. 4. RF board of the designed radar prototype.

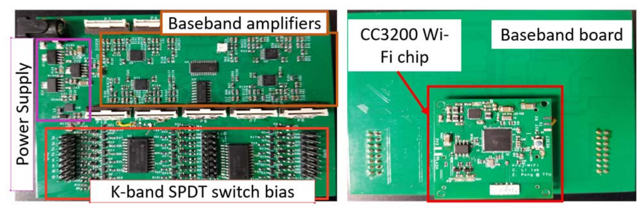

(a) (b)

Fig. 5. Baseband board of the radar prototype. (a) Baseband board front-side. (b) Wi-fi board connected on the back-side.

TABLE II. RADAR PARAMETERS OF THE PROTOTYPE DESIGNED

Parameter	**Value**
Sweep Bandwidth	240 MHz
Sweep Duration	10 ms
Center frequency	24.125 GHz
ADC sampling rate	250 ksps

A stochastic search method is used to find a non-uniform distribution of the 8-element linear array. The convex optimization program CVX [6] is used to evaluate 100,000 random non-uniform distributions using MATLAB. The stochastic search is used to find distribution and weighting values of the array to obtain minimum main lobe width and side-lobe level. Fig. 3 represents the best distribution for the non-uniform array among 100,000 random distributions, where $[x_1, x_2, x_3, x_4, x_5, x_6, x_7, x_8]$ are the positions of the array elements. Table I lists the weighting values of the array elements for the best distribution.

B. MIMO radar

In the proposed 16×16 MIMO radar, two sets of 8 non-uniformly spaced transmitting elements are placed on the two horizontal ends of the prototype as shown in Fig. 1. Similarly, two sets of 8 non-uniformly spaced receiving elements are placed on the two vertical ends of the prototype. The elements are distributed as per Fig. 3. The equivalent virtual array is a 16×16 non-uniform spaced array.

The circular patch antennas are tilted by 45º to align the polarization of the transmitting and receiving elements. PIN diodes are used to extend the number of transmitters driven by the output of the PLL. Each Tx output from the PLL drives four transmitting antennas. PIN diodes act as RF switches and are used to turn on/off the RF path to a transmitter. A bias circuit is used to bias the RF switch. A power divider is designed to split the LO signal from the PLL to the receiver down-converter as shown in Fig. 1.

In the proposed design, only a single transmitter and receiver is active at any given time. Time-division multiplexing (TDM) is used to scan through all the 256 virtual channels. TDM provides a trade-off between scanning time and hardware complexity. The proposed MIMO radar employs digital beamforming. Let $S_{(m,n)}(t)$ be the time-domain signal, where m, n are integers from 1 to 16 representing the transmitter channel and receiver channel, respectively. The time-domain signal is converted into frequency-domain $S_{(m,n)}(f_b)$ to obtain the beat frequency f_b. The range profile of each virtual array element $S_{(m,n)}(R)$ can be obtained using the formula:

$$R = Tcf_b/2B \quad (1)$$

where R is the target range, T is chirp repetition period, c is the speed of light, and B is the bandwidth of the chirp.

The range profile for a specific zenith angle (θ) and azimuth angle (φ) can be calculated from the above 256-channel range profile using the digital beamforming method:

$$P(\theta,\varphi,R) = w^T(\theta) \times S(R) \times w(\varphi) \quad (2)$$

where:

$$S(R) = \begin{bmatrix} S_{(1,1)}(R) & \cdots & S_{(1,16)}(R) \\ \vdots & \ddots & \vdots \\ S_{(16,1)}(R) & \cdots & S_{(16,16)}(R) \end{bmatrix} \quad (3)$$

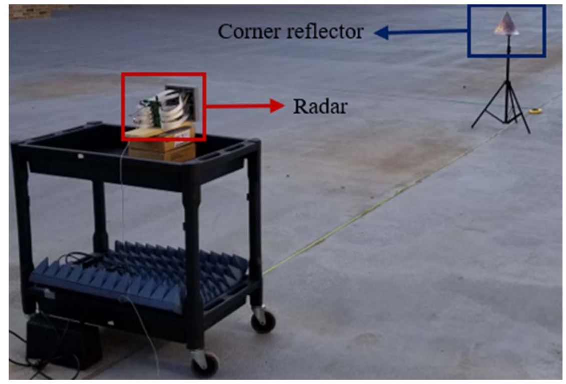

Fig. 6. Radar experiment setup.

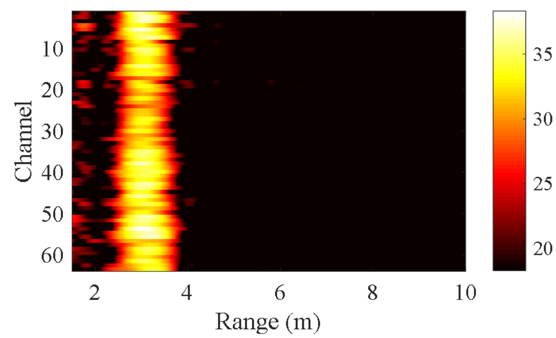

Fig. 7. Uncalibrated hot colormap range profiles of 64-channels for corner reflector placed at 3.2 m from radar.

$w(\theta)$ and $w(\varphi)$ are look-up tables of the weighting vectors generated using the convex optimization program discussed in Section II A.

III. Hardware Prototype and Experiment

The prototype consists of an RF front-end circuit and a baseband board. The radar prototype is designed for an angular resolution of 3º and side-lobe level of -10 dB. The RF circuit is built on a Rogers-3003 substrate with 0.254 mm thickness as shown in Fig. 4. The RF board consists of two 24-GHz radar transceiver chipsets from Analog Devices and a number of PIN diodes (MADP-000907-14020W) from MACOM. Each radar transceiver chipset consists of a PLL (ADF4159), a VCO (ADF5901), and two receiver down-converters (ADF5904). A 40 MHz clock (520L15IA40M0000) from CTS corporation acts as a common reference input to both the PLL's. The common reference input ensures coherence among different channels. The baseband board is built on an FR4 substrate and consists of power supply, 16-channel baseband amplifier, and bias circuits for PIN diodes as shown in Fig. 5 (a). A customized CC3200 Wi-Fi chip with built-in ARM-cortex M4 processor from Texas Instruments is connected on the back side of the baseband board as shown in Fig. 5 (b). The Wi-Fi chip acts as the controller for the radar. The RF and baseband boards are connected using flat cables and male-to-male connectors. The CC3200 chip has

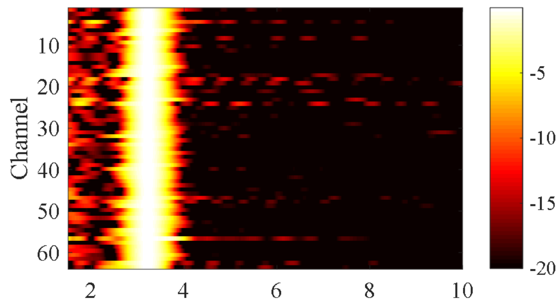

Fig. 8. Calibrated hot colormap range profiles of 64-channels for corner reflector placed at 3.2 m from radar.

a built-in ADC with four channels. Each channel provides a sampling rate of 62.5 ksps. To achieve a higher sampling rate, all the four channels are used together in the round-robin fashion, providing a sampling rate of 250 ksps. A 5-V supply is used to power the radar with an average power consumption of 2.5 W. Table II lists the key specifications. A Windows application was built using QT software to communicate with the radar. QT is a C++ cross-platform software development kit (SDK). The program uses transmission control protocol (TCP) to send commands to the radar board and user datagram protocol (UDP) to receive sampled baseband data. MATLAB is used for post-processing of the baseband data.

An experiment of short-range localization has been performed as shown in Fig. 6. A corner reflector was placed at a distance of 3.2 m from the radar. The radar is powered using a portable battery. Due to the coupling between the two PLLs on the RF board, only one PLL can be used at a time. This reduces the number of active transmitters and receivers to 8×8 at any given time. One full scan of the radar requires 0.64 seconds to collect 64-channel beat signals. Since the transmitters and receivers on the RF board have different path delays and component variation, a calibration method [7] is introduced in the signal processing stage to align the amplitude and phase response of all the receiver antennas for a given target.

In the calibration method introduced, the phase and amplitude of the received signals measured from the 64 channels are normalized and aligned to the phase and amplitude of the received signal measured from channel 0 (Tx0, Rx0 pair), which is used as the reference channel. Calibration is done by placing a corner reflector in front of the radar with centers aligned. The obtained calibration matrices will be used for future measurements. Fig. 7 represents the uncalibrated range profiles of 64-channels detecting a corner reflector located 3.2 m in front of the radar. Due to different path delay for each transmitter and receiver pair, the range information varies slightly. Fig. 8 represents the calibrated range profiles of the same 64-channels. Since the calibration aligns the amplitude and phase of the received signals to the reference channel, the range information obtained from each of the 64 channels matches. Any inaccuracy in range measurement by the reference channel results in slight inaccuracy in the calibrated range profiles of all the channels. The estimated range accuracy of the system is 5 cm. One way to improve the signal-to-noise ratio is by transmitting multiple chirps and averaging the time-domain signal corresponding to each chirp. The radar requires a scanning time of $16 \times 16T$ using a single-channel ADC where T is the chirp duration. The scanning time of the radar can be improved by using multiple-channel ADCs and reducing the chirp length.

IV. Conclusion

In this paper, the design and calibration of a portable 24-GHz 3-D MIMO FMCW radar were discussed. The design uses non-uniform spaced array along with MIMO to achieve higher angular resolution and 2-D beam scanning. A prototype was designed and implemented with 16 transmitter and 16 receiver channels. A calibration method was discussed to align the phase and amplitude of signals received by all antennas for a given target. Future work includes a more comprehensive calibration method to reduce clutter, collecting data from multiple chirps to improve signal-to-noise (SNR) ratio, and carrying out system level tests for 3-D imaging.

Acknowledgment

The authors would like to thank the National Science Foundation (NSF) for support under grants EECS-1808613 and CNS-1718483.

References

[1] H. J. Visser, *Array and Phased Array Antenna Basics*. Hoboken, NJ: John Wiley & Sons, 2006.

[2] R. Miura, T. Tanaka, I. Chiba, A. Horie, and Y. Karasawa, "Beamforming experiment with a DBF multibeam antenna in a mobile satellite environment " *IEEE Trans. Antennas Propag.*, vol. 45, no. 4, pp. 707-714, Apr. 1997.

[3] T. Geibig, A. Shoykhetbrod, A. Hommes, R. Herschel, and N. Pohl, "Compact 3D imaging radar based on FMCW driven frequency-scanning antennas " in *2016 IEEE Radar Conference, RadarConf 2016*, 2016, pp. 1–5.

[4] X. Zhuge and A. G. Yarovoy "A sparse aperture MIMO-SAR-based UWB imaging system for concealed weapon detection " *IEEE Trans. Geosci. Remote Sens.*, vol. 49, no. 1, pp. 509–518, Jul. 2011.

[5] D. Bleh *et al.* "W-band time-domain multiplexing FMCW MIMO radar for far-field 3-D imaging " *IEEE Trans. Microw. Theory Techn.*, vol. 65, no. 9, pp. 3474–3484, Feb. 2017.

[6] M. Grant, and S. Boyd "CVX: Matlab software for disciplined convex programming, version 2.1." *2012-09-27). http://cvxr. com/cvx* (2014).

[7] Z. Peng and C. Li "A Portable K-Band 3-D MIMO Radar with Nonuniformly Spaced Array for Short-Range Localization." in *IEEE Transactions on Microwave Theory and Techniques.*